Electronic Supplementary Information (ESI)

An Ultrasensitive Electrochemiluminescence Biosensor for Multiple Detection of microRNAs Based on a Novel Dual Circuit Catalyzed Hairpin Assembly

Yue Zhang, Xue Li, Ziqi Xu, Yaqin Chai, Haijun Wang, and Ruo Yuan**

Key Laboratory of Luminescence and Real-Time Analytical Chemistry (Southwest University), Ministry of Education, College of Chemistry and Chemical Engineering, Southwest University, Chongqing 400715, People's Republic of China

* Corresponding authors. E-mail: hjwang@swu.edu.cn; yuanruo@swu.edu.cn.

Tel.: +86-23-68252277; Fax: +86-23-68253172.

Experimental Section

Reagents and Materials. 1-Ethyl-3- [3- (dimethylamino)-propyl] carbodiimide hydrochloride (EDC), N-hydroxy succinimide (NHS), Mercaptoethanol (MCH) were purchased from Sigma-Aldrich Co. (St. Louis, MO, U.S.A.). N- (4-aminobutyl)-N-ethylisoluminol (ABEI), dopamine (DA), $Ru(bpy)_3Cl_2 \cdot 6H_2O$, Nafion (5%, *wt/wt*), $H_2Pt_2Cl_6 \cdot 6H_2O$, 3-thiophenemalonic acid (TA), and H_2O_2 were acquired from Suna Tech Inc. (Suzhou, China). The oligonucleotides (see Table S1) used in this work were synthesized and refined by Sangon Inc. (Shanghai, China). Human breast cancer cells (MCF-7) and cervical cancer cells (Hela) were purchased from the Type Culture Collection of the Chinese Academy of Sciences (Shanghai, China). In the meantime, the involved buffers were outlined as follows. DNA reserve buffer (pH = 8.0): 1×TE buffer (10 mM Tris-HCl, 1.0 mM EDTA). DNA annealing buffer and hybridization buffer (10 mM Tris-HCl, 1 mM EDTA, 15 mM $MgCl_2$, 200 mM NaCl, pH = 8.0). The detection phosphate buffer (PBS, pH = 7.0): 0.1 M Na_2HPO_4, 0.1 M KH_2PO_4, and 0.1 M KCl. 100 mM dithiothreitol (DTT). Deionized water was used throughout the experiment. All reagents were analytical grade and solutions were prepared using ultrapure water (specific resistance of 18 MΩ·cm).

Table S1. All DNA and miRNA Sequences Used in the Experiment

Name	Sequence (5′ to 3′)
MiRNA-21	UAG CUU AUC AGA CUG AUG UUG A

MiRNA-155	UUA AUG CUA AUC GUG AUA GGG GU
MiRNA-141	UAA CAC UGU CUG GUA AAG AUG G
MiRNA-let-7a	UGA GGU AGU AGG UUG UAU AGU U
Double-Hairpin H1	HS-TCAACATCAGTCTGATAAGCTACATTGGATGCTC TAGCTTATCAGACTGATGGACATGGATAATCGTGATA GGGGTTCCATGTCCATACCCCTATGAAGGAGCGACT
Hairpin H2	HOOC-TAAGCTAGAGCATCCAATGT AGCTTATCAGACTGCATTGGATGCTC
Hairpin H3	HOOC-TAATCGTGATAGGGGTATGGACAT GGAACCCCTATCACGATTAGCATTAAAGA

Instruments. In the whole experiment course, the three-electrode system which was made up of a modified glassy carbon electrode (GCE, Φ = 4 mm) as the working electrode, an Ag/AgCl electrode (sat. KCl) as the reference electrode, and a platinum wire as the auxiliary electrode was very necessary to accomplish the experimental detection.[1] The ECL measurement was conducted with a model MPI-A ECL analyzer (Xi′an Remax Electronic Science & Technology Co. Ltd., Xi′an, China). Cyclic voltammetry (CV) and electrochemical impedance spectroscopy (EIS) measurements were conducted with a CHI 660E electrochemical workstation (CH Instruments Inc.,

Shanghai, China). The scanning electron microscope (SEM, S-4800, Hitachi, Tokyo, Japan) was used to characterize the morphologies of the materials. The gel electrophoresis experimental measurements were carried out on the DYCP-31E electrophoresis apparatus (WoDeLife Sciences Instrument Co., Ltd., China).

Synthesis of Nafion-Ru-PtNPs. Nafion-Ru-PtNPs were synthesized based on the previous literature reports with a little modification.[2] Ru-PtNPs aggregates were prepared by blending the PtNPs colloid solution with $Ru(bpy)_3^{2+}$ aqueous solution. Firstly, PtNPs were prepared like follows. Briefly, 1 mL of 0.038 M H_2PtCl_6 aqueous solution was diluted to 50 mL with deionized water firstly, and then 0.5 mL of 0.3 M TA was slowly added into the solution. The solution was heated for 20 min at 100 ^oC with vigorous stirring until it turned into a dark brown solution. After that, 1 mL of 0.038 M $Ru(bpy)_3Cl_2$ aqueous solution was added into 50 mL of previously prepared colloidal PtNPs solution above slowly with vigorous stirring. PtNPs were firmly adsorbed by $Ru(bpy)_3^{2+}$, owing to the electrostatic interactions between positively charged $Ru(bpy)_3^{2+}$ and negatively charged PtNPs. Then, a large quantity of black aggregates occurred and precipitated, which proved that the preparation of Ru-PtNPs was successful. In order to enhance the film-forming properties, 1 mL Nafion solution (5%, *wt/wt*) was added into the obtained Ru-PtNPs solution under stirring and Nafion-Ru-PtNPs were prepared successfully.

Synthesis of H2·ABEI and H3·DA. Prior to use, the oligonucleotides of H2 and H3 were annealed at 95 ^oC for 5 min, then slowly cooled down to room temperature to form a hairpin structure. H2·ABEI and H3·DA were prepared by the following procedures

using NHS and EDC as the cross-linking agent. Firstly, COOH- modified H2 (5 μM) and H3 (5 μM) were activated for 2 h by 0.05 M NHS and 0.2 M EDC respectively. Then, 0.02 M ABEI solution and 0.02 M DA solution were added to the above mixture solution respectively, which were reacted at 4 ^{o}C overnight with stirring. Therefore, H2·ABEI and H3·DA were synthesized successfully. H2·ABEI and H3·DA were stored at 4 ^{o}C for later use.

Construction of the Proposed ECL Biosensor. The construction of ECL biosensor was showed in Scheme 1. Before modification, GCE needed to be pretreated as follows steps. First, GCE was polished carefully on the polishing cloth by using 0.3 and 0.5 μm alumina powder, respectively, with a silky feeling. After washing the remaining polishing powder on the surface of GCE, the ethanol and deionized water were used for ultrasonic cleaning three times respectively. Then, GCE was air-dried naturally to achieve a mirror-like surface. After drying in the air, the proposed ECL biosensor was fabricated on the cleaned GCE. First, 10 μL Nafion-Ru-PtNPs were dropped onto the GCE surface and dried at 37 ^{o}C for 1 h. Then, 10 μL H1 (1 μM) was incubated on the Nafion-Ru-PtNPs modified GCE surface at 4 ^{o}C for 12 h to ensure that H1 was immobilized on the material. And next, the modified GCE was blocked with 10 μL 1 mM MCH at room temperature for 50 min. Subsequently, in order to complete the first circuit, the electrode was further incubated with 10 μL H2·ABEI (1 μM) and 10 μL miRNA-21 at 37 ^{o}C for 2 h. In the presence of target 1 miRNA-21, a-hairpin of H1 was opened. Then miRNA-21 could be replaced by H2·ABEI, and the released miRNA-21 would attend the next cycle, which finally made a large amount of H2·ABEI be

immobilized on the electrode surface. Simultaneously, ABEI, as an effective energy donor, could greatly enhance the ECL signal of $Ru(bpy)_3^{2+}$ (energy acceptor), achieving significantly enhanced ECL signal (signal-on) and reaching sensitive detection of target 1. Following that, GCE was modified with 10 μL H3·DA (1 μM) and 10 μL miRNA-155 at 37 °C for 2 h to reach the second circuit. MiRNA-155 hybridized with b-hairpin of H1, and further could be displaced by H3·DA. And the released miRNA-155 was available for initiating next cycle, resulting in hundreds of duplexes (H1-H2·ABEI-H3·DA) formation on the electrode. There was a distinct decline of the ECL signal (signal-off) due to the ECL double quenching effect of DA for both ABEI and $Ru(bpy)_3^{2+}$, achieving sensitive detection of target 2. It was worth noting that each modification of a substance was required to clean the electrode with deionized water.

Experimental Procedures for Cell Analyses. To further verify the practical applicability of this proposed biosensor, we examined the expression of miRNA-21 and miRNA-155 in different biological cell lysates. And after consulting the relevant literature,[3-6] we selected human breast cancer cells (MCF-7) and cervical cancer cells (Hela) lysates as a comparison. First, the cell samples were processed by a commercial miRNA extraction kit after cell counting. Then, 10 μL Nafion-Ru-PtNPs were dropped onto the clean GCE surface and dried at 37 °C for 1 h. And next, 10 μL H1 (1 μM) was incubated on the Nafion-Ru-PtNPs modified GCE surface at 4 °C for 12 h to ensure that H1 was immobilized on the material. Subsequently, the modified GCE was blocked with 10 μL 1 mM MCH at room temperature for 50 min. For the first CHA process, the electrode was further

incubated with 10 μL H2·ABEI (1 μM) and 10 μL biological cell lysate of different cell numbers (0 to 10^5) at 37 °C for 2 h. Similarly, for the second CHA process, in order to ensure the accuracy of the miRNA-155 analysis, we introduced the maximum number of MCF-7 cells (10^5) in advance to complete the first CHA process. Following that, GCE was modified with 10 μL H3·DA (1 μM) and 10 μL biological cell lysate of different cell numbers (0 to 10^5) at 37 °C for 2 h to reach the second CHA process.

The Characterization of the PtNPs and Ru-PtNPs. We performed scanning electron microscopy (SEM) and UV-visible absorption spectra characterization of PtNPs and Ru-PtNPs. Firstly, SEM was performed to characterize the preparation of PtNPs and Ru-PtNPs, which was clearly showed in Figure S1 in the revised electronic supplementary information. Figure S1A showed that the PtNPs were spatially separated. However, as shown in Figure S1B, it could be clearly observed that the PtNPs were obviously aggregated after the formation of Ru-PtNPs complex. That was because PtNPs were firmly adsorbed by $Ru(bpy)_3^{2+}$ owing to the electrostatic interactions between positively charged $Ru(bpy)_3^{2+}$ and negatively charged PtNPs. And $Ru(bpy)_3Cl_2·6H_2O$ as a coordination compound reduced the conductivity of PtNPs, leading to the SEM of Ru-PtNPs were not brighter than that of PtNPs. The obtained results above illustrated the successful preparation of Ru-PtNPs, which were also consistent with the previously published literature.[7-9]

In addition, we also investigated the characteristics of Ru–PtNPs complex via UV-visible absorption spectra (Figure S2). All of these results indicated that the complex

was successfully synthesized and the results were consistent with the previously published literature.[7] The absorption spectrum of Ru-PtNPs (curve c) at 238 nm slightly red-shifted compared to that of PtNPs (curve a) at 232 nm, this could prove the π-π interactions between 3-thiophenemalonic acid (TA) and $Ru(bpy)_3^{2+}$, because the absorption band was red-shifted as the conjugation length increased.[10] The absorption spectrum of Ru-PtNPs (curve c) at 238 nm slightly blue-shifted compared to that of $Ru(bpy)_3^{2+}$ (curve b) at 244 nm, which could be attributed to the quantum size effect of PtNPs. Those changes proved that the Ru-PtNPs complex was successfully prepared.

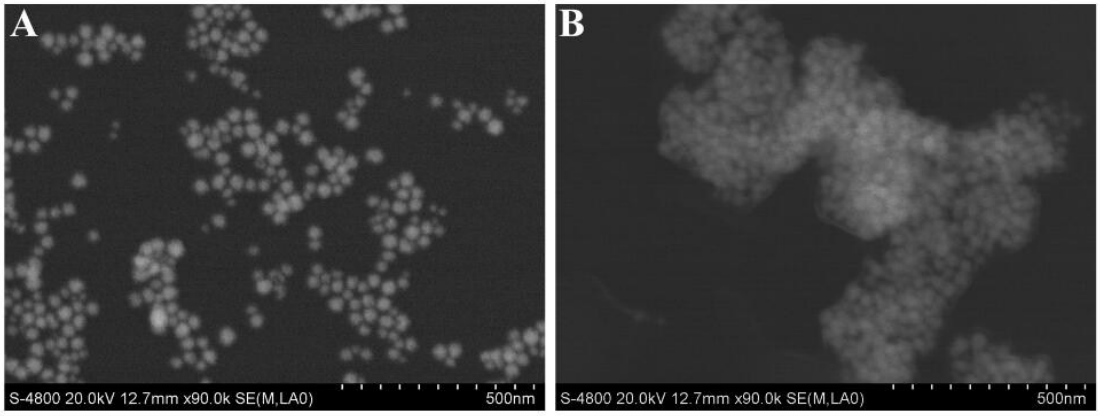

Figure S1. SEM image of (A) PtNPs and (B) Ru-PtNPs complex.

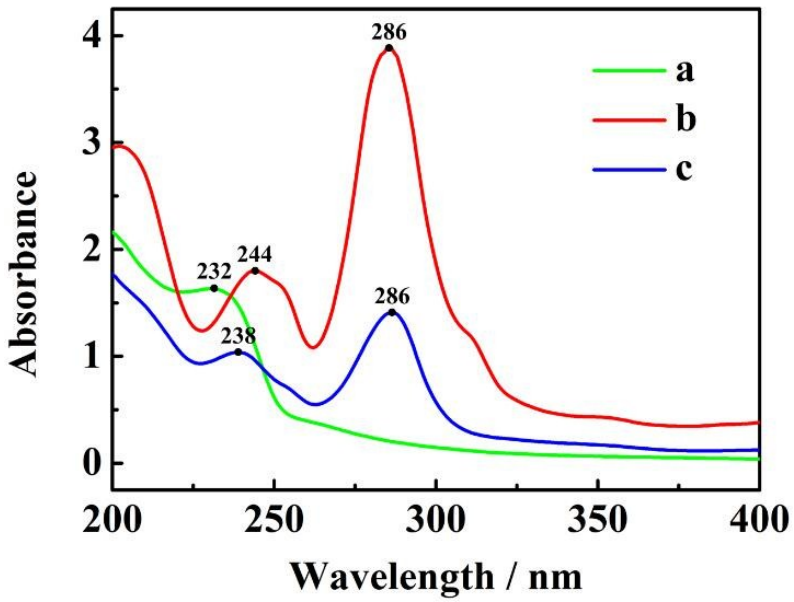

Figure S2. UV-visible absorption spectra of (a) PtNPs; (b) $Ru(bpy)_3^{2+}$; (c) Ru-PtNPs.

ECL and Electrochemical Characterization of the Proposed Biosensor. We used the model MPI-A ECL analyzer for characterization to demonstrate the successful preparation of the proposed biosensor. As depicted in Figure S3, the electrode was modified with Nafion-Ru-PtNPs, H1 and MCH, which had certain signal of the ECL intensity due to the ECL luminophore of $Ru(bpy)_3^{2+}$ (curve a). After the first circuit, ECL signal was significantly enhanced because of the ERET occurred during the reaction process. The a-hairpin of H1 was opened, resulting in the immobilization of a large amount of H2·ABEI on the electrode surface, and ECL signal of $Ru(bpy)_3^{2+}$ could be significantly enhanced by ABEI through energy transfer (signal-on, curve b). When the second circuit was completed, a sharp reduction of ECL signal was produced, because b-hairpin of H1 was opened, leading to the immobilization of a large amount of H3·DA on the electrode surface, and DA doubly quenched the luminescence of both $Ru(bpy)_3^{2+}$ and ABEI (signal-off, curve c). All ECL signals were measured in 2 mL PBS (0.1 M, pH = 7.0) by scanning the potential from 0.2 to 1.25 V at a scanning rate of 100 mV/s.

Furthermore, CV and EIS experiments were accomplished to characterize each step of the modification in 5.0 mM $[Fe(CN)_6]^{3-/4-}$ by scanning the potential from −0.2 to 0.6 V at a scan rate of 50 mV/s and in $[Fe(CN)_6]^{3-/4-}$ (5.0 mM) containing KCl (0.1 M). As seen in Figure S4A, a pair of notable $[Fe(CN)_6]^{3-/4-}$ redox peaks could be clearly observed on bare electrode (curve a). When the electrode surface was covered by a layer of Nafion-Ru-PtNPs successfully, the redox peaks

declined remarkably due to the inhibition effect of Nafion for electronic transmission (curve b). After H1 was incubated on the electrode, a decrease in redox current could be observed, because H1 blocked the transfer of electrons (curve c). Then the non-specific binding sites were blocked by MCH and the redox current was further reduced (curve d). After H2 and H3 were modified onto the electrode surface and combined with H1 respectively, the peak further declined, which was ascribed to the higher impedance brought about by the immobilization of nucleic acid (curve e and f). As shown in Figure S4B, a small semi-circle was observed for the electron transfers resistance (R_{et}) of bare GCE (curve a). After the modification of Nafion-Ru-PtNPs, the R_{et} increased distinctly, it showed that Nafion-Ru-PtNPs were successfully loaded on the electrode (curve b). When the H1, MCH, H2, and H3 were modified onto the GCE continuously, the R_{et} kept increasing and the reason was that the electron transfer was attenuated (curve c to f).

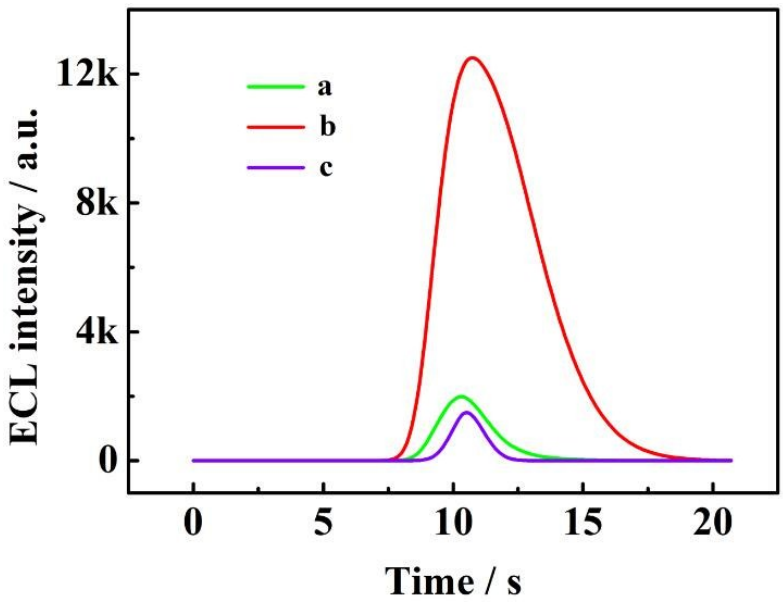

Figure S3. ECL-time diagram of the biosensor: (a) the initial signal of GCE/Nafion-Ru-PtNPs/H1/MCH, (b) signal-on state of GCE/Nafion-Ru-PtNPs/H1/MCH/ H2·ABEI (1 nM miRNA-21), (c) signal-off state of GCE/Nafion-Ru-PtNPs/H1/MCH/H2·ABEI/H3·DA (1 nM miRNA-155).

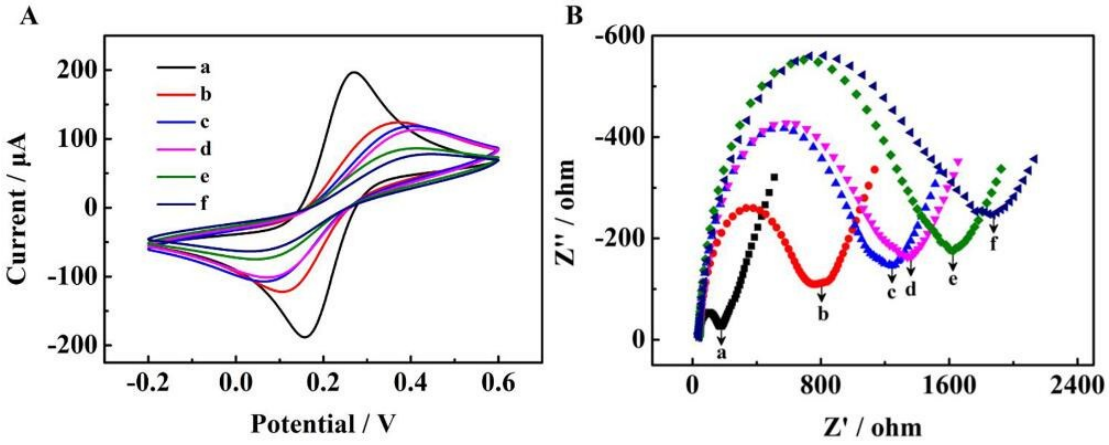

Figure S4. (A) CVs and (B) EIS at the (a) bare GCE, (b) GCE/ Nafion-Ru-PtNPs, (c) GCE/Nafion-Ru-PtNPs/H1, (d) GCE/Nafion-Ru-PtNPs/H1/MCH, (e) GCE/Nafion-Ru-PtNPs/H1/MCH/H2, (f) GCE/Nafion-Ru-PtNPs/H1/MCH/H2/H3 in 5.0 mM $[Fe(CN)_6]^{3-/4-}$ by scanning the potential from −0.2 to 0.6 V at a scan rate of 50 mV/s and in $[Fe(CN)_6]^{3-/4-}$ (5.0 mM) containing KCl (0.1 M).

Study of ERET between the ABEI and $Ru(bpy)_3^{2+}$. First, in order to prove the ERET between ABEI (energy donor) and $Ru(bpy)_3^{2+}$ (energy acceptor), the photoluminescence (FL) spectra of them was monitored. As seen from Figure S5, there was a distinct overlapping between the FL emission (E_m) spectrum of ABEI and the FL excitation (E_x) spectrum of $Ru(bpy)_3^{2+}$, demonstrating the great feasibility of ERET between ABEI (energy donor) and $Ru(bpy)_3^{2+}$ (energy acceptor).

In addition, ECL signal contrast experiments were further performed to prove that ABEI could provide energy to $Ru(bpy)_3^{2+}$, and the experimental results are shown in

Figure S6. When the electrode scanned in 2 mL PBS (0.1 M, pH = 7.0) containing the $Ru(bpy)_3^{2+}$ solution, a small ECL peak about 582.9 a.u. (curve a) was observed. However, an obvious higher ECL peak intensity (4146.7 a.u.) was obtained after adding the ABEI into the above solution (curve b) because of the ERET from the donor of ABEI to the acceptor of $Ru(bpy)_3^{2+}$.

Additionally, some references also reported the effective ERET between ABEI (energy donor) and $Ru(bpy)_3^{2+}$ or its derivatives (energy acceptor), based on which some sensitive biosensors were fabricated.[11-13]

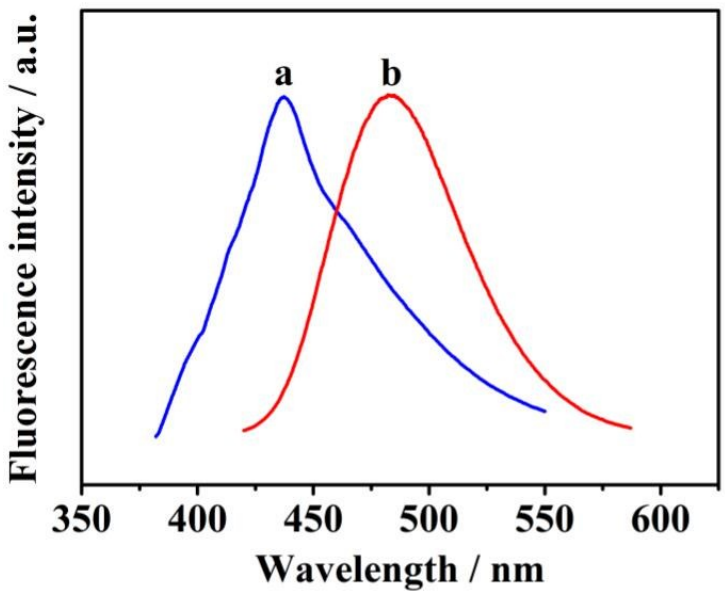

Figure S5. FL emission spectrum for ABEI (a) and FL excitation spectrum for $Ru(bpy)_3^{2+}$ (b).

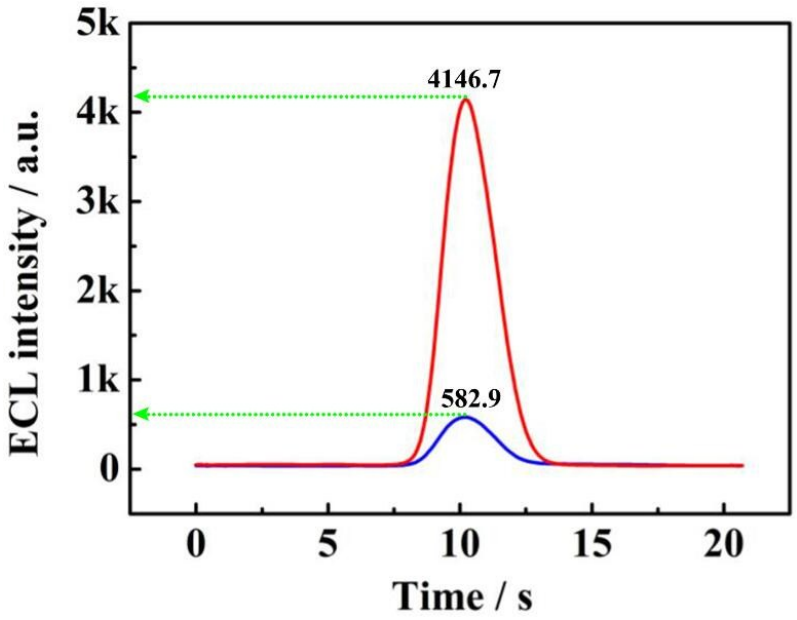

Figure S6. ECL curves of $Ru(bpy)_3^{2+}$ (a), ABEI and $Ru(bpy)_3^{2+}$ (b).

Study of the double quenching effect of DA. In order to verify the double quenching effect of DA to the ECL of ABEI and $Ru(bpy)_3^{2+}$, some supplementary experiments were also performed. At first, it has been reported that dopamine (DA) could quench the ECL signal of ABEI.[11,14] For further proving that, the ECL signals of the ABEI solution without and with DA were recorded. As seen from Figure S7A, a high initial ECL intensity was obtained (curve a) in the ABEI solution, while about 2892.7 a.u. decline of the ECL intensity was acquired when DA was added. In addition, it has also been proven that DA was a classic quencher to the ECL of $Ru(bpy)_3^{2+}$.[11,15] Similarly, a comparative experiment was also performed in the Ru complex solution. As shown in Figure S7B, about 4386.9 a.u. decline of the ECL intensity was acquired after the addition of DA to the Ru complex solution. The experimental results above demonstrated that DA had double quenching effect to the ECL of ABEI and $Ru(bpy)_3^{2+}$ in this work. The double quenching effect was further confirmed by obvious ECL changes in the fabricated process of the biosensor (seen from Figure S3).

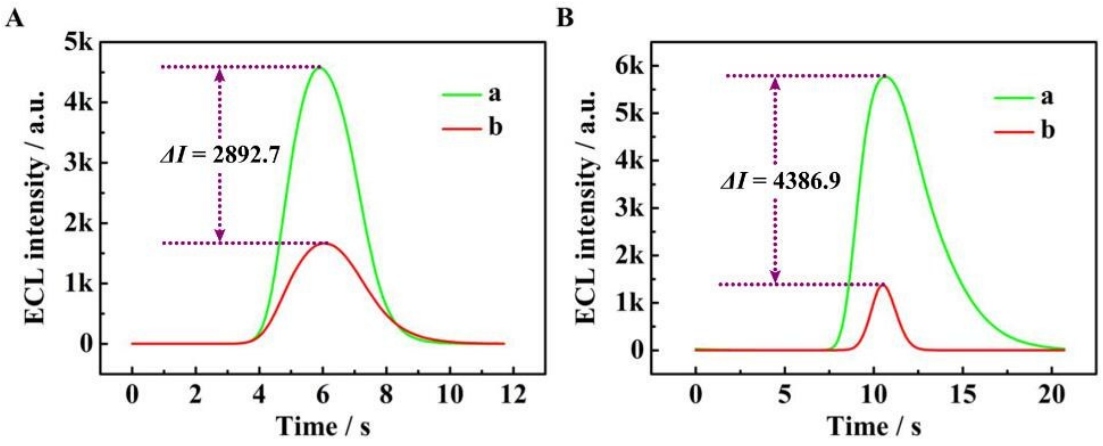

Figure S7. (A) ECL intensities of GCE in ABEI solution (a) and that in ABEI solution with the presence of DA (b). (B) ECL intensities of GCE in Ru complex solution (a) and that in Ru complex solution with the presence of DA (b).

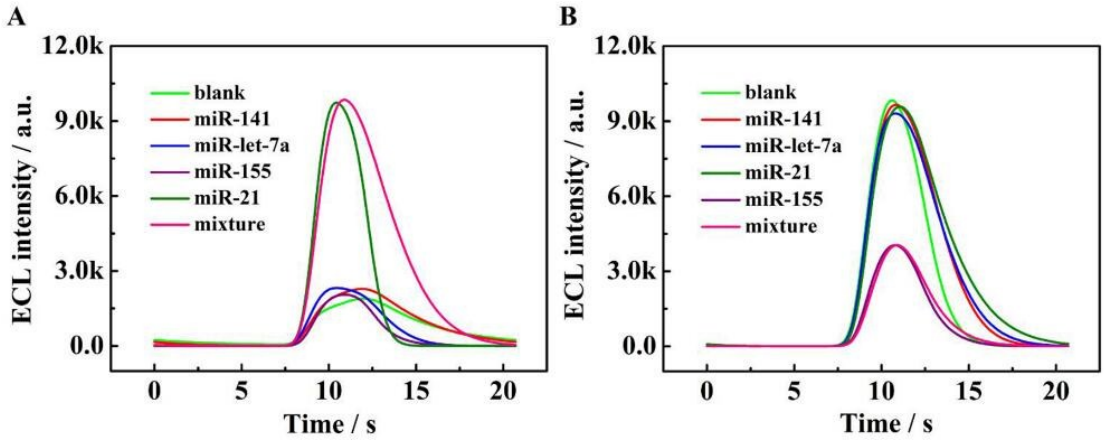

Figure S8. Selectivity of the miRNA biosensor with different targets: (A) blank, miRNA-141 (2 nM), miRNA-let-7a (2 nM), miRNA-155 (2 nM), miRNA-21 (20 pM), and the mixture containing miRNA-21(20 pM). (B) blank, miRNA-141 (2 nM), miRNA-let-7a (2 nM), miRNA-21 (2 nM), miRNA-155 (20 pM), and the mixture containing miRNA-155 (20 pM).

At the same time, this biosensor was compared with previous detection methods and strategies. As presented in Table S2, the biosensor demonstrated a higher sensitivity and lower detection limit than other methods in the detection of the miRNA.

Table S2. The Proposed Biosensor Compared with Other Works for miRNA Detection

Analytical methods	Linear range	Detection limit	Ref.
Fluorescence	2 nM to 60 nM	0.68 nM	16
Fluorescence	1 nM to 5 μM	0.3 nM	17
Electrochemical	5 pM to 0.5 fM	1.92 fM	18
Electrochemical	0.10 to 10.0 nM	5 pM	19
ECL	10 fM to 100 pM	3.3 fM	20
ECL	0.5 fM to 50 pM/1 fM to 50 pM	0.16 fM/0.33 fM	6
ECL	5.0 fM to 500 pM/5.0 fM to 500 pM	1.51 fM/1.67 fM	21
ECL	50 aM to 500 pM/20 aM to 1 nM	14.8 aM/5.3 aM	This work

References

1. X. Y. Jiang, H. J. Wang, H. J. Wang, Y. Zhuo, R. Yuan, Y. Q. Chai, *Anal. Chem.*, 2017, **89**, 4280−4286.

2. X. P. Sun, Y. Du, L. X. Zhang, S. J. Dong, E. K. Wang, *Anal. Chem.*, 2006, **78**, 6674–6677.

3. Y. J. Liu, J. N. Xiao, H. X. Lin, Y. L. Bai, X. B. Luo, Z. G. Wang, B. F. Yang, *Nucleic Acids Res*., 2009, **37**, e24.

4. S. J. Ye, X. X. Li, M. L. Wang, B. Tang, *Anal. Chem*., 2017, **89**, 5124−5130.

5. C. Feng, X. X. Mao, H. Shi, B. Bo, X. X. Chen, T. S. Chen, X. L. Zhu, G. X. Li, *Anal. Chem*., 2017, **89**, 6631−6636.

6. P. Zhang, Z. F. Lin, Y. Zhuo, R. Yuan, Y. Q. Chai, *Anal. Chem.*, 2017, **89**, 1338−1345.

7. Y. He, Y. Q. Chai, R. Yuan, H. J. Wang, L. J. Bai, Y. L. Cao, Y. L. Yuan, *Biosens. Bioelectron.*, 2013, **50**, 294–299.

8. B. B. Kou, Y. Q. Chai, Y. L. Yuan, R. Yuan, *Anal. Chem.*, 2017, **89**, 9383−9387.

9. B. B. Kou, L. Zhang, H. Xie, D. Wang, Y. L. Yuan, Y. Q. Chai, R. Yuan, *ACS Appl. Mater. Interfaces*, 2016, **8**, 22869−22874.

10. D. M. Richard, T. N. Stephanie, P. W. Shawn, D. L. Renae, J. Manikandan, *J. Am. Chem. Soc.*, 1993, **115**, 4910-4911.

11. H. J. Wang, L. Y. Peng, Y. Q. Chai, R. Yuan, *Anal. Chem.*, 2017, **89**, 11076−11082.

12. Y. Chen, S. W. Zhou, L. L. Li, J. J. Zhu, *Nano Today*, 2017, **12**, 98−115.

13. J. L. Liu, M. Zhao, Y. Zhuo, Y. Q. Chai, R. Yuan, *Chem. Eur. J.*, 2017, **23**, 1853 – 1859.

14. P. Zhang, X. Y. Wu, R. Yuan, Y. Q. Chai, *Anal. Chem.*, 2015, **87**, 3202-3207.

15. Q. Li, J.Y. Zheng, Y. L. Yan, Y. S. Zhao, J. N. Yao, *Adv. Mater.*, 2012, **24**, 4745-4749.

16. J. T. Yi, T. T. Chen, J. Huo, X. Chu, *Anal. Chem.*, 2017, **89**, 12351−12359.

17. Z. M. Ying, Z. Wu, B. Tu, W. H. Tan, J. H. Jiang, *J. Am. Chem. Soc.*, 2017, **139**, 9779−9782.

18. K. Zhang, H. F. Dong, W. H. Dai, X. D. Meng, H. T. Lu, T. T. Wu, X. J. Zhang, *Anal. Chem.*, 2017, **89**, 648−655.

19. A. D. Castaneda, N. J. Brenes, A. Kondajji, R. M. Crooks, *J. Am. Chem. Soc.*, 2017, **139**, 7657−7664.

20. Z. Q. Xu, L. L. Liao, Y. Q. Chai, H. J. Wang, R. Yuan, *Anal. Chem.*, 2017, **89**, 8282−8287.

21. L. C. Peng, P. Zhang, Y. Q. Chai, R. Yuan, *Anal. Chem.*, 2017, **89**, 5036−5042.